



The characterization of mesoporous silica (Ms) supporting cerium carbonate (Ms-Ce) and its adsorption performance for defluorination in aqueous solutions

Lizhu Zhang^a, Wei Tan^b, Rui Wang^b, Yongjun Yang^b, Min Yang^{b,*}, Hongbin Wang^{b,*}

^aSchool of Ethnic Medicine, Yunnan Minzu University, Kunming, Yunnan, 650500, P.R. China, email: 365157842@qq.com (L.Z. Zhang)

^bKey Laboratory of Resource Clean Conversion in Ethnic Regions, School of Chemistry and Environment, Yunnan Minzu University, Kunming, Yunnan, 650500, P.R. China, email: 317366182@qq.com (W. Tan), 392639402@qq.com (R. Wang), 1060656032@qq.com (Y.J. Yang), 826677468@qq.com (M. Yang), wanghb2152@126.com (H.B. Wang)

Received 1 March 2018; Accepted 113 October 2018

ABSTRACT

In this paper, the mesoporous silica (denoted as Ms) was modified by cerium and the optimum preparation conditions were investigated for cerium loaded mesoporous silica materials (denoted as Ms-Ce). The Ms-Ce materials for the fluoride removal performance were characterized by using SEM, XRD, FT-IR and TG-DTA. The Ms-Ce had good defluorination performance due to its large surface area and good-dispersive effect. The results show that cerium is successfully loaded onto the surface of the Ms and the structure of Ms did not change during the loading process. The defluorination loading by Ms-Ce can reach 75.54% under the optimum conditions ($n\text{NaHCO}_3/n\text{Ce} = 3.0$, $n\text{Ce}/n\text{Si} = 0.08$ and 90°C drying temperature). The adsorption performance and capacities of Ms-Ce were investigated through adsorption kinetics and adsorption isotherm tests. The maximum fluorine removal efficiency on the loaded materials were that the adsorbent dosage, pH value and adsorption time. They were showed as 1.6 g/L, 3.0 and 240 min, respectively. Dynamics research results showed that the fluoride removal process conformed to pseudo-second order kinetic model. Isothermal adsorption results showed that the fluorine ion adsorption process of Ms-Ce was accord with the Langmuir isotherm adsorption model. The maximum adsorption capacity was 17.96 mg/g. The mainly reaction showed that the active component of cerium carbonate has completed ion exchange with fluoride ion to generate CeCO_3F .

Keywords: Mesoporous silica; Cerium carbonate; Fluoride removal

1. Introduction

Fluoride is one of essential trace element owing to its established role in biology and environmental science. With the rapid development of industry, the fluoride emissions are also increasing. Excessive intake of fluoride will bring harm to human body, it can result in fluorosis with “dental fluorosis” in light and skeletal fluorosis in severe cases, such as limb pain, joint stiffness, skeletal deformation, operational difficulties, cancer, brain injury, thyroid secretion disorders and even paralyzed death [1]. At present, there are many

methods to remove fluoride from industrial wastewater, such as adsorption, chemical precipitation, ion exchange, membrane separation, electroagglomeration and so on [2]. Among them, the adsorption method has the advantages of small secondary pollution, high efficiency, simple operation and safety, and is the most effective method for fluoride removal. The adsorbents commonly used in water treatment included activated carbon, ion exchange resin and silica gel [3]. However, a single adsorbent can not completely remove pollutants from water. Therefore, the adsorbents have good adsorption effect becomes particularly important.

*Corresponding author.

Presented at the 10th International Conference on Challenges in Environmental Science & Engineering (CESE-2017), 11–15 November 2017, Kunming, China

Mesoporous silica (Ms) has uniform pore size, high specific surface area, good biocompatibility, easy modification and good stability. It is widely used in photochemistry, electrochemistry, biological materials, medicine, catalysis, adsorption, separation, other functional materials and other fields. Rare earths are widely distributed in the earth's crust, China's rare earth reserves top and rich variety in the world [4]. Therefore, they can effectively remove inorganic ions in water, such as fluoride, phosphorus, arsenic, ammonia nitrogen, chromium, cadmium and other pollutants by adsorption.

In this paper, the co-precipitation method was used to prepare the composite adsorbent material of Ms-Ce, it has high adsorption rate and large adsorption capacity. The effects of pH, temperature and adsorbent dosage on the adsorption of F⁻ were investigated, and the adsorption kinetics and adsorption isotherms were studied. It provides some new ideas and theoretical support in the field of studying fluoride ion adsorption.

2. Experiment

2.1. Materials and reagents

Hexon nitrate hexahydrate (Ce(NO₃)₃·6H₂O 98%) purchasing from Tianjin Institute of Fine Chemical Industry, China; Sodium fluoride (NaF 98%) purchasing from Chengdu Chemical Reagent Factory, China; sodium bicarbonate (NaHCO₃) and sodium nitrate (NaNO₃) purchasing from Tianjin Damao Chemical Reagent Factory, China; All the reagents were analytical grade.

2.2. Preparation of Ms

Ms was synthesized using the method reported by Li, et al. [5]. The surface area, total pore volume and average pore size are 1363 m²/g, 0.876 cm³/g and 3.30 nm respectively.

2.3. Preparation of Ms-Ce

Cerium as a modifier of Ms, with a certain amount mole ratio of Ce/Si, cerium was dissolved in silica dispersion solution, and then the precipitant of Na₂CO₃ was slowly added to the above mixed solutions under the stirring condition. After continuously stirring for 10 h, it was filtered, washed and dried, the Ms-Ce had been successfully prepared.

In order to study the effect of the NaHCO₃/Ce molar ratio on the adsorption performance, 0.3 g of Ms-Ce dispersed in 30 mL of deionized water, 0.1 molar ratio of Ce/Si rare earth metal salts was added into the above solution and dissolved in the mixed dispersion solution after stirring, 30 mL of different molar ratios of NaHCO₃/Ce (1.5, 2.0, 3.0, 4.0, 5.0 and 6.0) solution were added dropwise into the above solution and stirred continuously for 10 h, then filtered, washed and dried at 90°C in vacuum.

In order to investigate the molar ratio of Ce/Si on the adsorption performance, 30 mL of different mole ratio of Ce/Si (0.02, 0.04, 0.06, 0.08, 0.10, 0.08 and 0.10) solutions were used to prepare Ms-Ce composites under optimum preparation conditions.

In order to investigate the effects of calcination temperature on the adsorption performance, Ms-Ce composites pre-

pared under optimum conditions were calcinated (at 90°C, 200°C, 300°C, 400°C, 500°C, 600°C and 700°C) to obtain the temperature effects on the removal of fluoride.

2.4. Evaluation method

2.4.1. Analysis method

The determination method for fluorine ion content is in accordance with the "water and water quality monitoring analysis method" (GB7484-1987) of the ion selective electrode method [6].

2.4.2. Adsorption experiment

Adsorption experiments were carried out by batch adsorption method in a condition of 25°C in a shaker at 200 rpm for 3 h. 0.1000 g of Ms-Ce was added into conical flask. 50 mL of 10 mg/L fluoride ion solution (F⁻) was transferred in this bottle. After centrifugal separation, the residual concentration of fluoride ion in the supernatant fluid was determined. The removal rate R (%) and adsorption capacity Q (mg/g) were used to evaluate the performance of Ms-Ce materials.

The removal rate of R (%) is:

$$R(\%) = \frac{C_0 - C_t}{C_0} \times 100\% \quad (1)$$

The adsorption capacity of Q (mg/g)

$$Q(\text{mg} \cdot \text{g}^{-1}) = \frac{(C_0 - C_t) \times V}{m \times 1000} \quad (2)$$

The initial concentration of fluoride ion (mg/L) in the wastewater is C₀; the residual concentration of fluoride ion (mg/L) in wastewater is C_t; the adsorbent for fluoride ion adsorption capacity (mg/g) is Q; the amount of fluoride ion solution (mL) is V; the adsorbent amount (g) is M.

2.5. Characterization of the changes of the Ms-Ce before and after adsorption

SEM, XRD, FT-IR, TG-DTA was used to investigate the changes of the Ms-Ce before and after adsorption, and the adsorption mechanism was explained. Morphology of prepared materials were observed on scanning electron microscopy (FEI-Nova, NanoSEM450, America). The structures of the materials were characterized by XRD (Rigaku, Japan) with Cu Ka radiation (45 KV, 250 mA) and a continuous scan mode was employed with a scan rate of 10° min⁻¹. Fourier transform infrared spectroscopy (FT-IR) were obtained by a spectrometer (NICOLETIS10) with the powder samples embedded in KBr disks. The prepared materials were analyzed by Thermogravimetric analyzer (TG-DTA, STAA49F31, Germany)

2.6. Experimental study on static defluorination performance of Ms-Ce

2.6.1. Effect of adsorbent dosage on fluoride adsorption

Adsorption experiments were carried out in a shaking table in a condition of 25°C and the speed of 200 rpm for

3 h. Different dosage (0.1–4.0 g/L) of Ms-Ce was added into adsorption bottle, and 50 mL of 10 mg/L fluoride ion solution (F^-) was added to this bottle. After centrifugal separation, the residual concentration of fluoride ion in the supernatant fluid was determined

2.6.2. Effect of adsorption time on the fluoride adsorption

The above optimal adsorbent dosage was added into adsorption bottle, and transferred 50 mL of 10 mg/L fluoride ion solution (F^-) in this bottle. Adsorption experiments were carried out at different times from 10 to 300 min, as well, by following the same steps mentioned above.

2.6.3. Effect of initial solution pH on the fluoride adsorption

The above optimal adsorbent dosage was added into adsorption bottle, and 50 mL of 10 mg/L of fluoride ion solution (F^-) in this bottle whose range of pH was 2–12. After centrifugal separation, the residual concentration of fluoride ion in the supernatant fluid was determined.

2.7. Kinetic and adsorption isotherms studies

Adsorption experiments using a shaking table at different temperature conditions (25°C, 35°C, 45°C) and the speed of 200 rpm for 3 h. The above optimal amount of adsorbent was added into adsorption bottle, and transferred 50 mL of fluoride ion solution (F^-) in this bottle whose concentration was 2–80 mg/L, as well, by following the same steps mentioned earlier. The adsorption kinetics were fitted and drawn by the quasi-first-order kinetic and quasi-second-order kinetic adsorption models. The adsorption isotherms were plotted and drawn by using Langmuir adsorption model and Freundlich adsorption model.

3. Results and discussion

3.1. Preparation conditions selection

3.1.1. The effect of precipitating agent on the adsorption of F^-

In order to study the effect of precipitation agents on the adsorption performance, Ms was modified by the precipitant of $NaHCO_3$, NH_4HCO_3 , $NH_3 \cdot H_2O$ and Na_2CO_3 . The modified fluorine removal rate is shown in Fig. 1. We can see that the materials prepared by different precipitation agents had great effect on the removal rate of fluoride ions. Especially, $NH_3 \cdot H_2O$ as a precipitating agent, the removal rate of less than 20%, while the other three precipitant removal rate are more than 70%. The preparation process was not easy to control when Na_2CO_3 was as a precipitation agent, it easily produce alkali carbonate. In addition, NH_4HCO_3 as precipitator, it can cause that solution to be present NH_4^+ , and then secondary pollution [7]. So finally $NaHCO_3$ was chosen as the precipitant, and it can eliminate the effect of ammonia nitrogen produced by the precipitation process of ammonium bicarbonate..

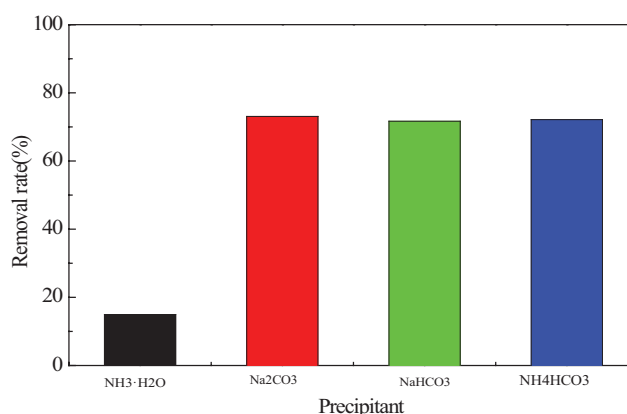


Fig. 1. Different precipitants on the effect of fluoride removal.

3.1.2. Effect of different $nNaHCO_3/nCe$ molar ratio on the adsorption of F^-

In order to investigate the effects of different molar ratios of $NaHCO_3/Ce$ on the adsorption of F^- , the effect of molar ratio of $NaHCO_3/Ce$ (1.5, 2.0, 3.0, 4.0, 5.0 and 6.0) on fluoride ion removal was investigated and the results were shown in Fig. 2. It can be seen from the Fig. 2 that $nNaHCO_3/nCe$ has little effect on the removal of fluoride ions. The main reason may be that the rare earth Ce can be completely precipitated when the molar ratio was more than 3.0, however, the rare earth Ce cannot be completely precipitated when the molar ratio was less than 3.0. And therefore the molar ratio of Ce/Si was less than the theoretical value of 0.1, it still has good effect to remove fluoride ion. In order to ensure that Ce was precipitated completely and have a better adsorption performance, the molar ratio of $NaHCO_3/Ce$ was chose as 3.0.

3.1.3. Effect of different molar ratio of Ce/Si on the adsorption of F^-

The effect of the molar ratio of Ce/Si on the adsorption of F^- is shown in Fig. 3. We can see that the removal efficiency gradually increased when the molar ratio of Ce/Si from 0.02 to 0.08, the removal rate was stable when the molar ratio was 0.08, the removal rate has not changed substantially when the molar ratio was more than 0.08. If the Ce content increased excessively, it led to its excessive overlay on the Ms and existed alone [8], thus the Ce cannot be fully utilized. The mole ratio of Ce/Si was chose as 0.08.

3.1.4. Effect of calcination temperature on the adsorption of F^-

In order to study the effect of calcination temperature on the adsorption of F^- , the effect of calcination temperature on the F^- removal is shown in Fig. 4. As can be seen from Fig. 4, the removal rate can reach about 80% at the calcination temperature of 90°C, and then the calcination temperature continues to increase, the removal rate reduced sharply to 30% and finally only 20%. It shows that the calcination temperature has a great influence on the adsorption material of Ms-Ce. The reason may be that the adsorption material of crystal structure was destroyed at high temperature

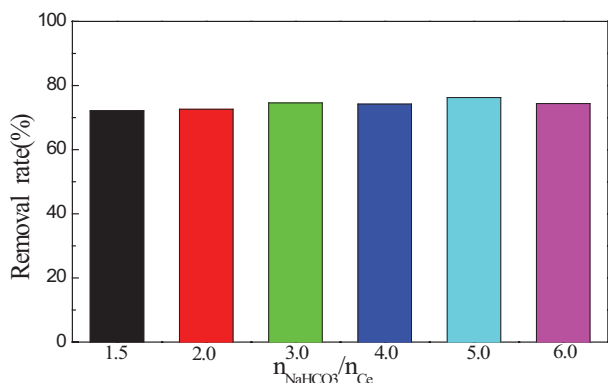


Fig. 2. Effect of mole ratio of NaHCO₃ /La on the removal of fluoride.

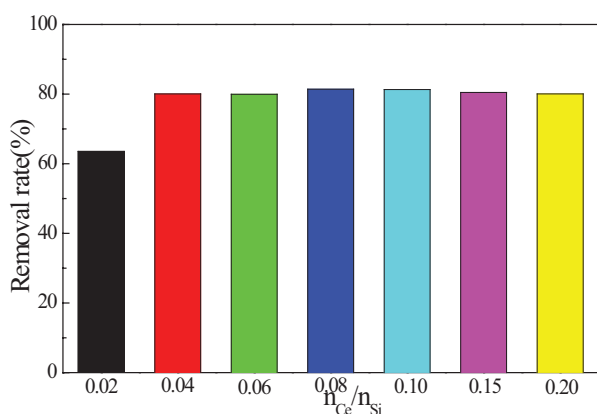


Fig. 3. The molar ratio of Ce/Si on the removal of fluoride.

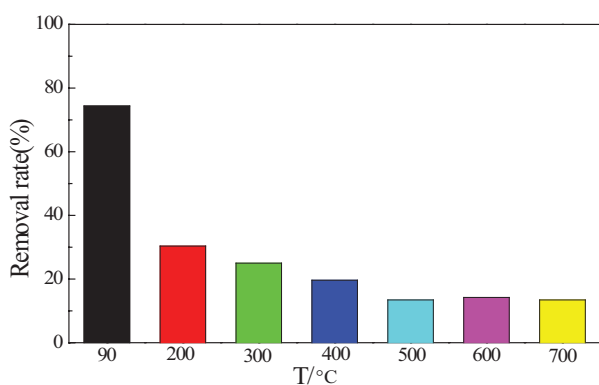


Fig. 4. Effect of different calcination temperature on the removal rate for fluoride.

[9], which leads to the decrease of adsorption performance. In this study, the temperature was selected as 90°C.

Based on the above data analysis and discussion, the optimum preparation conditions of adsorbent were: NaHCO₃ as precipitant, $n_{\text{NaHCO}_3}/n_{\text{Ce}} = 3.0$, $n_{\text{Ce}}/n_{\text{Si}} = 0.08$, calcination temperature = 90°C in vacuum. The preparation process is as follows: the 0.375 g of Ms dispersed in 30 mL deionized water, adding a certain amount of cerium

nitrate, and stirred until it is fully dissolved, and then 20 mL of NaHCO₃ solution was dropped into the above solution, and stirred continuously for 10 h at speed of 200 rpm. Then the adsorbent was filtered, washed and dried at 90°C in vacuum overnight.

3.2. Characterization of Ms-Ce

3.2.1. SEM analysis

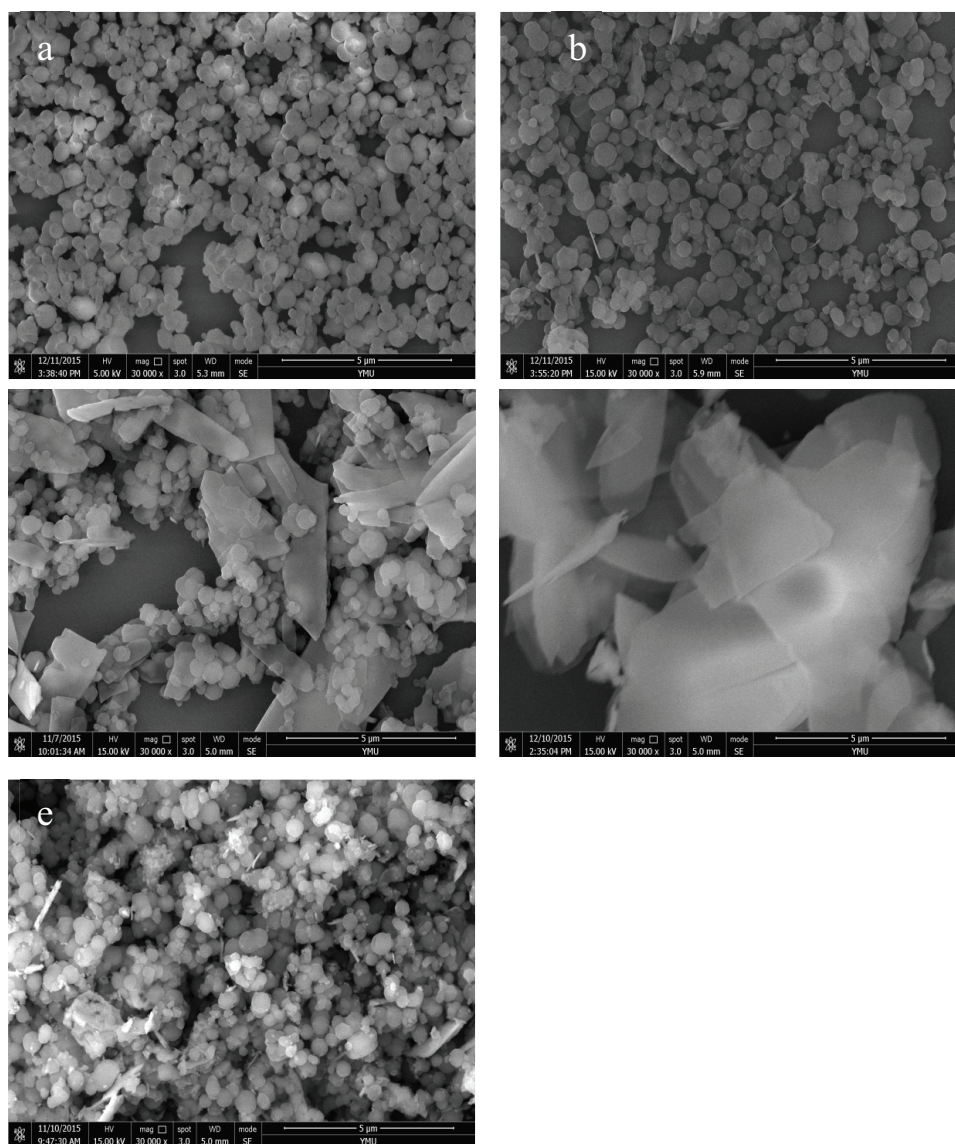
The SEM images of the different molar ratios of Ce/Si (0.02, 0.08 and 0.20), pure-Ce₂(CO₃)₃ and Ms-Ce at Ce/Si ratio of 0.08 after adsorption is shown in Fig. 5. The SEM images of pure-Ce₂(CO₃)₃ can be seen from Fig. 5d, it is sheet accumulation. According to Figs. 5a–c, with the increase of Ce/Si molar ratio, the sheet accumulation of material of Ms-Ce continues to increase seriously. It can be seen that it has a small amount of cerium carbonate on the surface of Ms-Ce when the molar ratio of Ce/Si was 0.02 from Fig. 5a. Sheet material significantly increased on the surface of Ms, and the degree of accumulation and deposition became higher when the molar ratio of Ce/Si was 0.2 (Fig. 5c). This is due to the fact that the cerium carbonate it cannot be completely coprecipitated on the surface of Ms or into the channels. Due to the degree of accumulation of Ms-Ce too high, F⁻ of solution cannot fully contact with the adsorbent, the active site of the adsorbent cannot be fully utilized [10]. It can be reflected the effect of fluoride removal, with the increase of the content of cerium carbonate, the effect of removal F⁻ was lower. Compared with Fig. 5b and Fig. 5e, the shape of Ms-Ce after adsorption changed obviously, the original small amount of sheet deposits basically disappeared, and small white particles were formed from Fig. 5e. This indicated that adsorption agents and adsorbates may react in the adsorption process.

3.2.2. XRD analysis

The XRD patterns of the pure-SiO₂ carrier, pure-Ce₂(CO₃)₃ and the composite material (Ms-Ce) is shown in Fig. 6. We can see that the Ms-Ce still remained the characteristic diffraction peaks of Ce₂(CO₃)₃ and had no shift. The content of Ce₂(CO₃)₃ was less, so peak intensity has been reduced compared with pure-Ce₂(CO₃)₃. The reason may be that some channels of Ms could have been blocked, and crystal structure was also weakened, but the mesoporous structure was not damaged during the preparation process [11].

The XRD patterns of the Ms-Ce treated at different calcination temperatures is shown in Fig. 7. We can see from Fig. 7, the characteristic peaks of Ce₂(CO₃)₃ disappeared and new diffraction peaks appeared at $2\theta = 18.16^\circ, 24.96^\circ, 31.03^\circ, 47.88^\circ, 54.793^\circ$, etc correspond to the standard card JCDP34-0394 when the calcination temperature of 200°C. After that, the diffraction peak became stronger and stronger with the increase of calcination temperature. It is no the new diffraction peak and becoming steady at the calcination temperature of 500°C. This indicates that the material has begun to decompose into CeO₂ at 200°C.

The XRD patterns of the material before and after adsorption are shown in Fig. 8. It can be seen from Fig. 8 that the diffraction peak of the Ms-Ce obviously changed



a:Ce/Si=0.02 b:Ce/Si=0.08; c:Ce/Si=0.20;d: Pure- $\text{Ce}_2(\text{CO}_3)_3$;e: after adsorption(Ce/Si=0.08)

Fig. 5. SEM images of different La/Si molar ratio.

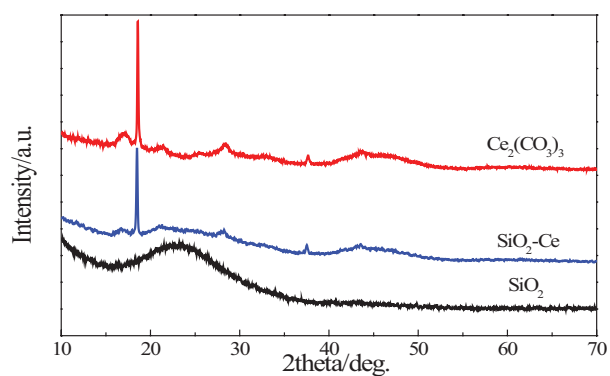


Fig. 6. The XRD spectra of Ms (SiO_2 carrier), pure- $\text{Ce}_2(\text{CO}_3)_3$ and Ms-Ce (SiO_2 -Ce).

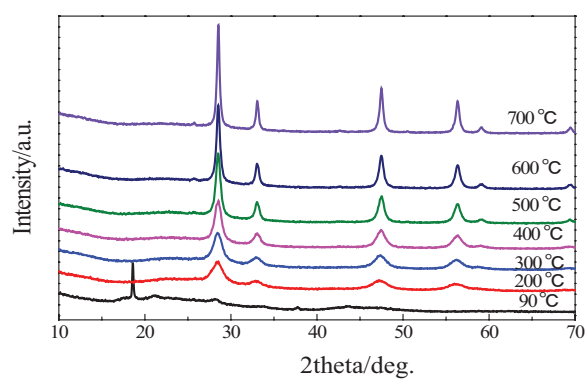


Fig. 7. The XRD spectra of Ms-Ce at different calcination temperatures.

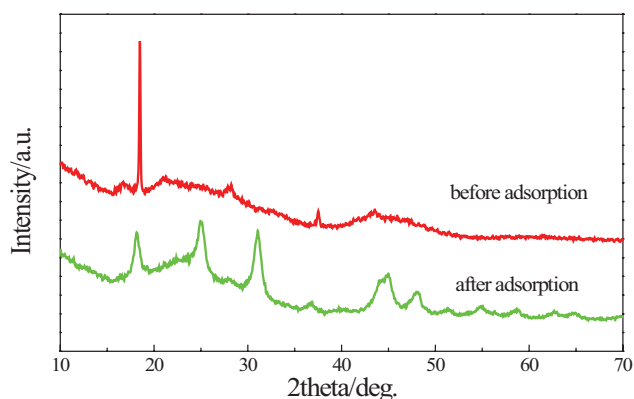


Fig. 8. The XRD spectra of the adsorbent before and after adsorption.

after adsorption, The major diffraction peaks located at $2\theta = 28.55^\circ, 33.08^\circ, 47.47^\circ$ and 56.33° which coincides with the standard card JCDP11-0340, indicating that the new material $\text{Ce}_2(\text{CO}_3)_3\text{F}$ was form after the adsorption, in addition there was a new diffraction peak which showed that a small amount of CeF_3 was generated [12].

3.2.3. FTIR analysis

The FTIR spectra of SiO_2 (a), Pure- $\text{Ce}_2(\text{CO}_3)_3$ (d) and SiO_2 -Ce before (b) and after (c) adsorption is shown Fig. 9. It can be seen that the adsorption peaks were mainly the characteristic peaks of Ms at 545, 1081, 1640 and 3438 cm^{-1} from Fig. 9a, the characteristic peaks of Pure- $\text{Ce}_2(\text{CO}_3)_3$ at 1440, 1081, 859, 741 and 681 cm^{-1} , in which the absorption peak at 859 and 1081 cm^{-1} was the frequency of the non-degenerate vibration absorption of carbonate. And it generally indicates the presence of a non-equivalent carbonate ion [13].

It can be seen that Ms-Ce before the adsorption still retained the characteristic peaks of cerium carbonate and silicon dioxide from Fig. 9b. The FITR spectra of the composites of Ms-Ce changed small, the most significant change was the enhancement absorption peak at 1440 cm^{-1} , the enhancement and broadening absorption peak at 1081 cm^{-1} , which was mainly caused by the introduction of cerium carbonate. According to Fig. 9c, the two characteristic peaks of Ms-Ce before the adsorption at $1440\text{--}1081\text{ cm}^{-1}$ had changed into a peak after adsorption [14].

The FITR spectra of the composite of Ms-Ce at different calcination temperature treatments are shown in Fig. 10. It can be seen that the calcined material still remained the characteristic peak of Ms. There are no new absorption peak in the FITR spectra of the material of Ms-Ce after the calcination temperature of 300°C , and the three strong absorption peak changed a wide peak at at 1440, 1081 and 860 cm^{-1} . The main reason was that $\text{Ce}_2(\text{CO}_3)_3$ was generated into $\text{Ce}_2\text{O}_2\text{CO}_3$ at high temperature. At temperatures above 500°C , the absorption peaks at 1081 cm^{-1} are enhanced. The reason was that the characteristic peaks of the carbonate gradually disappeared with the temperature continued to increase. $\text{Ce}_2(\text{CO}_3)_3$ was generated into Ce_2O_3 at high temperature.

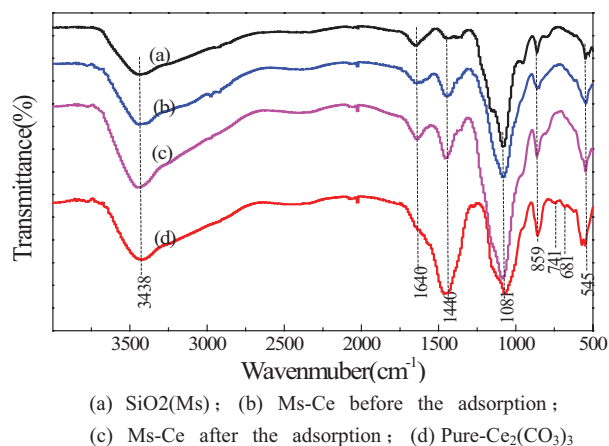


Fig. 9. The FTIR spectra of SiO_2 , Pure- $\text{Ce}_2(\text{CO}_3)_3$ and Ms-La before and after the adsorption.

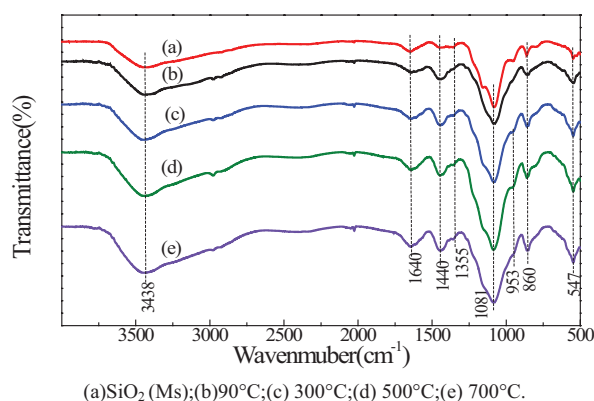


Fig. 10. Infrared spectra of the adsorbent at different calcination temperature.

3.2.4. TGDTA analysis

The TGDTA analysis of the composite of Ms-Ce before fluoride removal is shown in Fig. 11. The content of cerium carbonate was 23.47% in the Ms-Ce composite material. The first stage of the weight loss ratio was 12.79%, which was the loss of adsorbed water and crystal water. The second stage of the weight loss ratio of 6.98%, Ms-Ce lost two CO_2 molecules generated CeO_2 , and the weight loss ratio of 6.98% was consistent with the theoretical value of 6.51%. The TGDTA analysis of the composite of Ms-Ce after fluoride removal is shown in Fig. 12. Compared with Figs. 11 and 12, the main process is that CeCO_3F decomposed into CeOF_3 , and the weightlessness rate was 5.87%. Due to the decrease of carbonate content, the second weight loss stage after adsorption was smaller than that of before adsorption [15].

3.3. Study on static adsorption properties of Ms-Ce

3.3.1. Effect of adsorbent dosage on fluoride adsorption

In the process of experiment, the fluoride ion removal rate gradually increased as the dosage of adsorbent material increased, the removal rate of F^- increased rapidly with

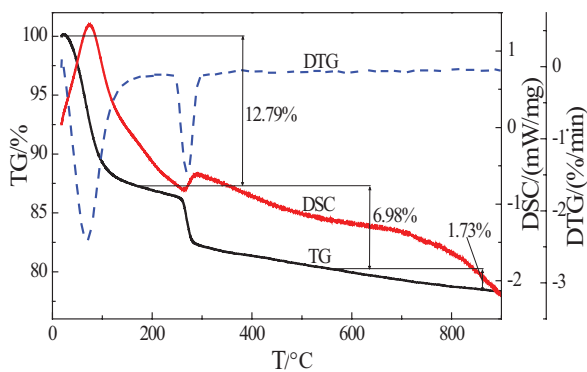


Fig. 11. TG-DTA analysis of Ms-Ce before the adsorption.

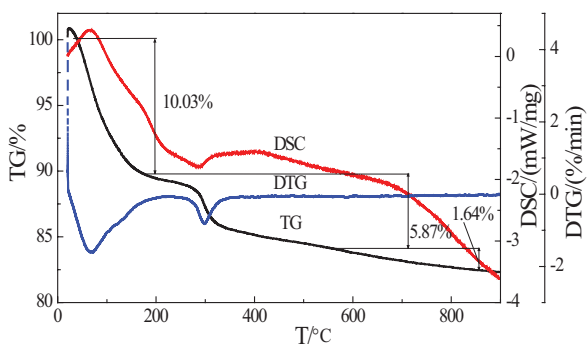


Fig. 12. TG-DTA analysis of Ms-Ce after the adsorption.

the increase of the dosage of Ms-Ce which was in the range of 0.1–0.8 g/L. The removal rate was up to 80% when the adsorbent dosage was 1.6 g/L, and then the removal rate increased slowly and tended to be gentle. The change of adsorbent dosage decreased slowly when adsorbent was more than 2.0 g/L. Therefore, 1.6 g/L adsorbent dosage was selected as optimal dosage.

3.3.2. Effect of adsorption time on fluoride adsorption

The effects of adsorption time and the initial F^- concentration of 10, 30 and 50 mg/L on adsorption performance of Ms-Ce are shown in Fig. 13. We can see that the adsorption process accelerated quickly in the first half, and adsorption tended to be slow down in the second half. The reason is that there were the higher concentration of F^- and the more effective sites of adsorbent at the beginning of adsorption. As the adsorption process went on, the concentration of F^- gradually decreased, the site was gradually occupied [16]. At different initial concentrations, the adsorption capacity of fluoride adsorbing on the adsorption material increased quickly at first, and then tended to be stable at the initial stage of adsorption. In order to that the adsorption process to reach the maximum balance. Hence, the adsorption time was 240 min.

3.3.3. Effect of initial solution pH on fluoride adsorption

The effect of the initial solution pH on the F^- removal is shown in Fig. 14, we can see that the material of Ms-Ce

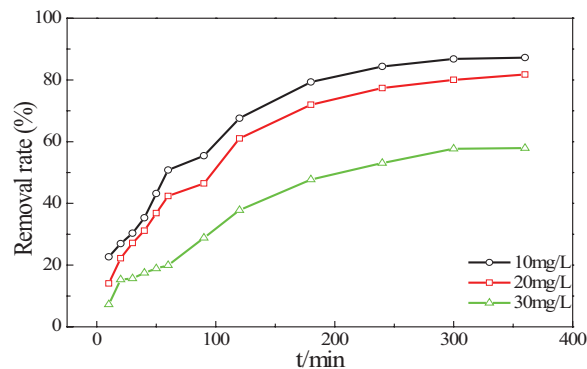


Fig. 13. Effect of different concentrations of time.

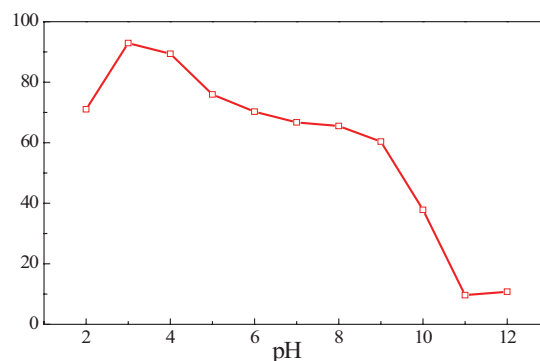


Fig. 14. Effect of initial solution pH on the removal of fluoride.

on the F^- removal have a wide range from 2.0 to 9.0, the removal rate of F^- increased with the increase of pH in the range of 2.0–3.0, The removal rate can reach to 92.94% and the concentration of F^- of solution was 0.71 mg/L in the pH value of 3.0. The removal rate of F^- gradually decreased slowly When the pH value was higher than 3.0, it may be that the increase of pH caused that the adsorbent surface potential decreased and adsorption agent surface had negatively charge [17], so it had repulsive effect on F^- and reduced fluoride removal effect. The removal rate gradually decreased slowly with the increase of pH in the range of 5.0 ~ 9.0. The removal rate was about 60% in the pH value of 9.0. As the pH value continues to increase, the removal rate decreased sharply and only 10%, the main reason was that under alkaline conditions, OH^- and F^- formed competitive adsorption, which reduced the number of active sites adsorbing fluoride ions, resulting in the reduction of fluoride removal efficiency [18]. Therefore, the pH value of 3.0 was selected as the optimal pH.

3.4. The analysis on the adsorption mechanism

3.4.1. Study on the adsorption kinetics

In order to explore the mechanism of the adsorption process, the adsorption kinetics was studied. There were also a lot of dynamic adsorption models, but the most popular dynamic models are quasi-first-order and quasi-second-order kinetic models [19].

The pseudo-first-order kinetic equation is as follows:

$$\log(Q_e - Q_t) = \log Q_e - k_1 t \tag{3}$$

The pseudo-second-order kinetic equation is as follow:

$$\frac{t}{Q_t} = \frac{t}{Q_e} + \frac{1}{k_2 Q_e^2} \tag{4}$$

Q_e is the adsorption capacity at adsorption equilibrium (mg/g); Q_t is the adsorption capacity at t (min) of adsorption time (mg/g); t is adsorption time (min); K_1 is the quasi-level adsorption rate constant (min^{-1}); K_2 is quasi-secondary adsorption rate constant [g/(mg·min)].

In the experiment, the experimental data at different temperatures (25°C, 35°C and 45°C) and initial concentrations (10, 30 and 50 mg/L) were fitted by two kinetic models [Eqs. (1) and (2)] [20], and the results were shown in Table 1. We can be seen from Table 1 that the linear fitting correlation coefficient of quasi-second-order kinetic model was greater than 0.9453, and was larger than that of quasi-first-order. This indicated that the quasi-second-order kinetic model can better describe the adsorption behavior of Ms-Ce on F⁻ in water. The kinetic fitting results at different temperatures showed that the correlation coefficient of the adsorption process at different temperatures was greater than 0.9891, it showed that the quasi-second-order kinetic adsorption model can also better describe the adsorption behavior.

3.4.2. Adsorption isotherm

Langmuir model and Freundlich model are two commonly used models in most of the adsorption isotherm studies to describe the adsorption thermodynamics of a liquid-solid system [21]. The Langmuir adsorption isotherm is as follows:

$$\frac{C_e}{Q_e} = \frac{1}{K_L Q_m} + \frac{C_e}{Q_m} \tag{5}$$

The Freundlich adsorption isotherm is as follows:

$$Q_e = K_f C_e^{1/n} \tag{6}$$

Q_m is the saturated adsorption capacity (mg/g); Q_e is the capacity at equilibrium adsorption (mg/g); K_L and K_f is adsorption equilibrium constant, C_e is the adsorption mass concentration at adsorption equilibrium (mg/L) and n is related to the temperature constant.

The experimental data at different temperatures is shown in Table 2. The fitting results show that the adsorption process of Ms-Ce on fluoride ion was more consistent with Langmuir isotherm model than that of the Freundlich isotherm model, the correlation coefficient R was greater than 0.9890, the maximum adsorption capacity was 17.96 mg/g. The comparison of Q_m with some other adsorbents (Table 3) also suggests that the Ms-Ce should be a good medium for the treatment of fluoride contaminated water.

Table 1
The correlation coefficients of quasi-first order kinetics equation and quasi-second order kinetics equation

Variable	Measured Q_e (mg/g)	Quasi-first order kinetics equation			Quasi-second order kinetics equation			
		Q_e (mg/g)	K_1/min^{-1}	R^2	Q_e (mg/g)	$K_2/(\text{g}\cdot\text{mg}^{-1}\cdot\text{min}^{-1})$	R^2	
$C_F/(\text{mg/L})$	10	5.453	2.935	0.0109	0.8048	6.498	0.00243	0.9891
	20	10.221	3.680	0.0094	0.7575	12.612	0.00099	0.9905
	30	10.859	4.274	0.0103	0.8043	15.110	0.00051	0.9453
T/K	298	5.453	2.935	0.0109	0.8048	6.498	0.00243	0.9891
	308	5.766	2.932	0.0128	0.6920	6.319	0.00497	0.9984
	318	5.595	1.469	0.0074	0.5899	5.811	0.01191	0.9990

Table 2
Isothermal adsorption model and its related fitting parameters

T/K	Langmuir isotherm model				Freundlich isotherm model			
	Equation	Q_{max} (mg/g)	K_L (L/mg)	R^2	Equation	$1/n$	K_F	R^2
298	$Q_e = \frac{4.1098C_e}{1 + 0.236C_e}$	17.397	0.236	0.9890	$Q_e = 3.598C_e^{0.4248}$	0.4248	3.598	0.8774
308	$Q_e = \frac{5.8837C_e}{1 + 0.328C_e}$	17.960	0.328	0.9922	$Q_e = 4.248C_e^{0.4028}$	0.4028	4.248	0.8754
318	$Q_e = \frac{3.8837C_e}{1 + 0.222C_e}$	17.027	0.222	0.9920	$Q_e = 3.272C_e^{0.4445}$	0.4445	3.272	0.9266

Table 3
Comparative assessment of research and other fluoride adsorbent

Adsorbent	Adsorption capacity (mg/g)	Ref.
GAC	4.12	[22]
GAC-AA	9.23	[22]
GAC-PH	10.42	[22]
Cellulose	2.42	[23]
La-Ch	4.008	[24]
Chitosan-praseodymium complex	15.87	[25]
Zeolite fly ash(ZFA)	14.30	[26]
Ms-Ce	17.96	This work

3.4.3. Adsorption mechanisms

Compared with Fig. 5b and Fig. 5e, the shape of Ms-Ce after adsorption changed obviously, the original small amount of sheet deposits basically disappeared, and small white particles were formed from Fig. 5e. This indicated that adsorption agents and adsorbate may react in the adsorption process, and a new material has formed. The material was mainly cerium carbonate before adsorption, part of the carbonate was replaced by F^- to form a new material $Ce(CO_3)F$ during the adsorption process. Mechanism of fluoride removal by the Ms-Ce belongs to the typical ion exchange adsorption [27,28], which may be expressed as follows:



where Ms is a carrier of SiO_2 .

4. Conclusion

In conclusion, we have successfully prepared the adsorption material of Ms-Ce by co-precipitation method. Moreover, the optimization of preparation conditions of Ms-Ce has been studied. It was found that the optimal preparation conditions of $nNaHCO_3/nCe$, nCe/nSi and drying temperature were 3, 0.08, and $90^\circ C$, respectively, and the removal rate of fluoride ion was up to 75.54%. The results showed that rare earth elements are attached to the mesoporous silica by cerium carbonate. The Ms has a large specific surface area and rich channel, so it can improve the dispersion of rare earth compounds and increase the active points and effective contact area of Ms-Ce compared with pure- $Ce_2(CO_3)_3$. The kinetic results showed that quasi-second-order kinetic model can better describe the adsorption behavior of fluoride on water. The results of isothermal adsorption showed that the adsorption of Ms-Ce on fluoride ion was more in accordance with the Langmuir isothermal adsorption model, the effect of temperature on adsorption was small, so it can be used to remove F^- from water at room temperatures, the correlation coefficient was greater than 0.9890 and the maximum adsorption capacity was 17.96 mg/g. The Ms-Ce material can be further applied to the removal of fluoride ions in the water.

Acknowledgements

This study was supported by Innovative projects for College Students of Yunnan Minzu University (2017JWC-DC-42) and National College Students' innovation and entrepreneurship Project (201610691002).

References

- [1] H. Yamashita, M. Okazaki, K. Ikeue, M. Anpo, Photocatalytic reduction of CO_2 with H_2O on ti-containing mesoporous silica hydrophobically modified using fluoride ions, *Stud. Surf. Sci. Catal.*, 153 (2004) 289–294.
- [2] J. Fan, D. Li, W. Teng, J. Yang, Y. Liu, L. Liu, Ordered mesoporous silica/polyvinylidene fluoride composite membranes for effective removal of water contaminants, *Mater. Chem. A.*, 4 (2016) 3850–3857.
- [3] L. Fang, F.P. Zhang, Y.X. Jing, J.T. Han, Research on the phosphate removal by consolidated and oxidized lanthanum, *Ind. Water Treat.*, 6 (2010) 11–14.
- [4] Z.J. Ma, B.C. Li, Experimental study on the modification of natural zeolite with fluoride removal by, *J. Silicate Bull.*, 33 (2014) 7–8.
- [5] Z.J. Li, B. Hou, Y. Xu, Preparation and characterization of silica-modified titanium dioxide nanoparticles by co-precipitation method, *Acta. Phys. Chim. Sin.*, 2 (2005) 229–233.
- [6] L.J. Zhang, X. Hu, C.Z. Yu, R. Crawford, Y. Aimin, Preparation of sinapinaldehyde modified mesoporous silica materials and their application in selective extraction of trace Pb(II), *J. Environ. Chem. A.*, 18 (2013) 9312–9317.
- [7] H.B. Wang, M. Yang, J. Wang, Phosphorus adsorption properties of adsorbent of load the lanthanum humic acid, *Rare Metal.*, 5 (2002) 356–359.
- [8] T. Wei, G.Z. Li, T.L. Wang, M. Yang, J.H. Peng, C.J. Barrow, W.R. Yang, H.B. Wang, Preparation and adsorption of phosphorus by new heteropolyacid salt-lanthanum oxide composites, *Desal. Wat. Treat.*, 57 (2016) 7874–7880.
- [9] W.F. Han, M. Yang, S.Y. Li, G.Q. Fang, H.B. Wang, On the adsorption of Lonicera on bentonite, *J. Yunnan Nation. Univ. (Natural Sci. Ed.)*, 4 (2008) 343–346.
- [10] Y. Wei, L.I. Shiliang, X. Yang, W.U. Yanping, An experiment on zeolite modified by cerium and its use for fluoride removal from drinking water, *Shenyang Jianzhu Univ.*, 29 (2013) 144–149.
- [11] K. Mukhopadhyay, A. Ghosh, S.K. Das, B. Show, P. Sasikumar, U.C. Ghosh, Synthesis and characterisation of cerium (iv)-incorporated hydrous iron (iii) oxide as an adsorbent for fluoride removal from water, *RSC Adv.*, 7 (2017) 26037–26051.
- [12] J.X. He, M.Y. Cui, Y.Y. Zheng, Self-assembly of modified silica nanospheres at the liquid/liquid interface, *Mater. Lett.*, 64 (2010) 463–465.
- [13] S.S. Dash, M.K. Sahu, E. Sahu, R.K. Patel, Fluoride removal from aqueous solutions using cerium loaded mesoporous zirconium phosphate, *New J. Chem.*, 39 (2015) 7300–7308.
- [14] M.J. Haron, W.M. Yunus, Removal of fluoride ion from aqueous solution by a cerium-poly(hydroxamic acid) resin complex, *J. Environ. Sci. Health Part A Toxic/Hazard. Substan. Environ. Eng.*, 36 (2001) 727–734.
- [15] J. Min, J.K. Park, E.W. Shin, Lanthanum functionalized highly ordered mesoporous media: implications of arsenate removal, *Micropor. Mesopor. Mater.*, 75 (2004) 159–168.
- [16] L. Chen, Granulation of Fe-Al-Ce nano-adsorbent for fluoride removal from drinking water by spray coating on sand in a fluidized bed, *Powder Technol.*, 193 (2009) 59–64.
- [17] X.Y. Fang, G.Z. Li, J. Li, V. Jegatheesan, H.B. Wang, M. Yang, Bamboo charcoal derived high-performance activated carbon via microwave irradiation and koh activation: application as hydrogen storage and super-capacitor, *Desal. Water Treat.*, 96 (2017) 120–127.
- [18] Z.J. Duan, G.Z. Li, L. Zhou, H. Gui, W. Tan, Preparation of zeolite-based zirconium functional materials (Ze-Zr) with the aid of response surface methodology, *Proc. Saf. Environ. Protect.*, 112 (2017) 353–361.

- [19] A. Benhouria, M.A. Islam, H. Zaghouane-Boudiaf, M. Boutahala, B.H. Hameed, Calcium alginate-bentonite-activated carbon composite beads as highly effective adsorbent for methylene blue, *Chem. Eng. J.*, 270 (2015) 621–630.
- [20] C. Tiar, M. Boutahala, A. Benhouria, H. Zaghouaneboudiaf, Synthesis and physicochemical characterization of ZnMg-NiAl-CO₃-layered double hydroxide and evaluation of its sodium dodecylbenzenesulfonate removal efficiency, *Desal. Water Treat.*, 57 (2016) 13132–13143.
- [21] Z. Wang, D.M. Fang, Q. Li, L.Z. Xia, Y. Zhu, H.Y. Qu, Y.P. Du, Modified mesoporous silica materials for on-line separation and preconcentration of hexavalent chromium using a micro-column coupled with flame atomic absorption Spectrometry, *J. Anal. Chim. Acta.*, 24 (2012) 725–735.
- [22] K.G. Rekha, R. Radhika, T. Jayalatha, S. Jacob, R. Rajeev, Removal of perchlorate from drinking water using granular activated carbon modified by acidic functional group: adsorption kinetics and equilibrium studies, *Proce. Saf. Environ. Protecty.*, 109 (2017) 158–171.
- [23] C.P. Sekhar, S. Kalidhasan, V. Rajesh, N. Rajesh, Bio-polymer adsorbent for the removal of malachite green from aqueous solution, *Chemosphere*, 77 (2009) 842–847.
- [24] K.B. Li, X.L. Tang, L. Guo, T. Zhang, Study on adsorption performance for fluoride by chitosan supported lanthanum, *J. Hunan Univ. Sci. Technol.*, 24 (2009) 113–117. (In Chinese)
- [25] E. Kusriani, N. Sofyan, N. Suwartha, Chitosan-praseodymium complex for adsorption of fluoride ions from water, *J. Rare Earth.*, 33 (2015) 1104–1113.
- [26] B.A. Shah, A.V. Shah, H.D. Patel, Alkaline hydrothermal conversion of agricultural waste bagasse fly ash into zeolite: utilisation in dye removal from aqueous solution, *Int. J. Environ. Waste Manag.*, 7 (2011) 192–208.
- [27] R. Wang, G. Li, Y. Yang, L. Shu, V. Jegatheesan, H.B. Wang, M. Yang, Study on the adsorption performance for fluoride by mesoporous silica loaded rare earth lanthanum (Ms-La) material, *Desal. Water Treat.*, 96 (2017) 104–111.
- [28] R. Wang, L. Luo, L. Shu, V. Jegatheesan, H.B. Wang, M. Yang, Preparation and characterization of mesoporous silica (Ms) supporting lanthanum carbonate (Ms-La) for the defluorination of aqueous solutions, *Desal. Water Treat.*, 96 (2017) 112–119.